Memory effect versus exchange bias for maghemite nanoparticles

K. Nadeem [a],*, H. Krenn [b], D.V. Szabó [c]

[a] *Materials Research Laboratory, Department of Physics, International Islamic University, Islamabad, Pakistan*
[b] *Institute of Physics, Karl-Franzens University Graz, Universitätsplatz 5, A-8010 Graz, Austria*
[c] *Karlsruhe Institute of Technology, Institute for Applied Materials, 76344 Eggenstein-Leopoldshafen, Germany*

A B S T R A C T

We studied the temperature dependence of memory and exchange bias effects and their dependence on each other in maghemite (γ Fe_2O_3) nanoparticles by using magnetization studies. Memory effect in zero field cooled process in nanoparticles is a fingerprint of spin glass behavior which can be due to i) surface disordered spins (surface spin glass) and/or ii) randomly frozen and interacting nanoparticles core spins (super spin glass). Temperature region (25 70 K) for measurements has been chosen just below the average blocking temperature ($T_B = 75$ K) of the nanoparticles. Memory effect (ME) shows a non monotonous behavior with temperature. It shows a decreasing trend with decreasing temperature and nearly vanishes below 30 K. However it also decreased again near the blocking temperature of the nanoparticles e.g., 70 K. Exchange bias (EB) in these nanoparticles arises due to core/shell interface interactions. The EB increases sharply below 30 K due to increase in core/shell interactions, while ME starts vanishing below 30 K. We conclude that the core/shell interface interactions or EB have not enhanced the ME but may reduce it in these nanoparticles.

1. Introduction

The magnetic memory effect in nanoparticles has been investigated intensively due to its complex behavior [1 3]. Memory and aging effects are considered as finger prints for spin glass behavior in magnetic systems [4 8]. Spin glass arises in magnetic systems due to randomness and frustration of magnetic spins. There can be two kinds of spin glass behavior in nanoparticles, one is the super spin glass [9 11] which arises in interacting nanoparticles due to random freezing of the huge core spin (super spin) of individual nanoparticles, while second is the surface spin glass in core/shell nanoparticles due to disordered surface spins [12,13]. The memory effect (ME) is reported also for non interacting superparamagnetic nanoparticles due to distribution in their relaxation times which arises through particle size distribution [14]. Differentiation of ME due to particle size distribution and spin glass can be done by using zero field cooled (ZFC) and field cooled (FC) magnetic measurements. The ME due to particles size distribution of superparamagnetic nanoparticles can be found only in FC, while spin glass nanoparticles show ME in both ZFC and FC protocols. De et al. [15] studied the ME in nanocrystalline super paramagnetic $Fe_{50}Ni_{50}$ alloy embedded in silica matrix and observed ME in FC only, which arises due to particle size distribution.

Khan et al. [16] reported memory effect in ZFC process for $La_{0.9}Sr_{0.1}CoO_3$ single crystal and attributed it to spin glass behavior. Therefore in this article we have done ME in ZFC process to exclude the possibility of ME due to particle size distribution albeit the microwave plasma synthesis provides the most narrow size distribution among other preparation methods.

For interacting nanoparticles, the ME increases with increasing nanoparticle concentration (dipolar interactions) [17]. Peddis et al. [18] reported ME in super spin glass ferromagnetic (FM) Co nanoparticles in antiferromagnetic (AFM) Mn matrix and found that the ME increases with increasing nanoparticle concentration and interface interactions (between nanoparticles and matrix). Domingo et al. [19] reported exchange bias (EB) phenomena in the same super spin glass system (Co nanoparticles in Mn matrix). Malik et al. [20] reported ME in FC process for nickel ferrite/polymer composites and found suppression of ME with increasing magnetic nickel ferrite component in the composite. Vasilakaki et al. [21] did Monte Carlo simulation of the ME of an assembly of FM core/AFM shell nanoparticles and found good comparison with the experimental results of system containing FM Co nanoparticles dispersed in AFM Mn matrix. They concluded that both dipolar interactions and interface interactions increase the ME. ME has been also reported for non interacting core/shell nanoparticles which signifies the presence of surface spin glass freezing in them due to disordered spins at the nanoparticle's surface. Bisht et al. [12] reported ME in both ZFC and FC processes for nickel oxide nanoparticles and attributed it to surface spin glass behavior.

Unlike FM nanoparticles dispersed in AFM matrix, the interface interactions in bare ferrite nanoparticles are between surface spins and core spins. Core/shell interface interactions are dominate in fine sized nanoparticles due to large surface to volume ratio. These core/shell interactions in nanoparticles lead to the EB effect, which is well known for FM layers on AFM substrates [22–24]. Cabreira Gomes et al. [25] reported the presence of EB in core/shell $MnFe_2O_4/\gamma$-Fe_2O_3 and $CoFe_2O_4/\gamma$-Fe_2O_3 nanoparticles and attributed it to core/shell interactions. Therefore in this article, we have chosen fine 6 nm maghemite (γ-Fe_2O_3) spinel ferrite nanoparticles to extract possible correlation between memory and exchange bias effects by using temperature dependent magnetic measurements.

2. Experimental

γ-Fe_2O_3 nanoparticles were prepared by microwave plasma synthesis. The complete synthesis process and structural evaluation of the materials (made by the same synthesis process) is reported elsewhere [26,27]. Average particle size and size distribution statistics were determine from an image analysis of transmission electron micrographs (TEM, model number CM20 from FEI with 200 kV acceleration voltage and LaB6 cathode). Magnetic measurements were taken by using superconducting quantum interference device (SQUID) magnetometry (Quantum Design, MPMS XL 7). The AC susceptibility measurements were performed by the same magnetometer.

3. Results and discussion

Fig. 1 shows the transmission electron microscopy (TEM) image of maghemite nanoparticles at 10 nm scale. It is observed that the nanoparticles are nearly of spherical shape. Average particle size as calculated from log normal distribution function fit was 6.1 nm with a normalized standard deviation (σ_D)=0.22 [28].

Fig. 2(a) shows the ZFC/FC magnetization curves taken under applied field of 50 Oe. The ZFC curve exhibits peak at 75 K which corresponds to average blocking temperature (T_B) of the nanoparticles. Below T_B, the nanoparticles spins are blocked in their anisotropy (easy) axes and are in blocked state. Above T_B, nanoparticles spins get de blocked due to enough thermal energy and will be in superparamagnetic state [29]. The FC curve gets separated from ZFC and flattens below T_B. The flatness of the FC curve is an indication for the presence of spin glass behavior and/or interparticle interactions in these nanoparticles. In fine core/shell maghemite nanoparticles, the surface effects are more dominant
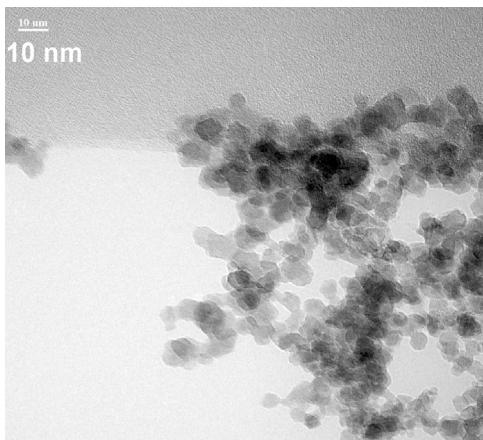

Fig. 1. Transmission electron microscopy image of fine 6 nm maghemite nanoparticles at 10 nm scale.
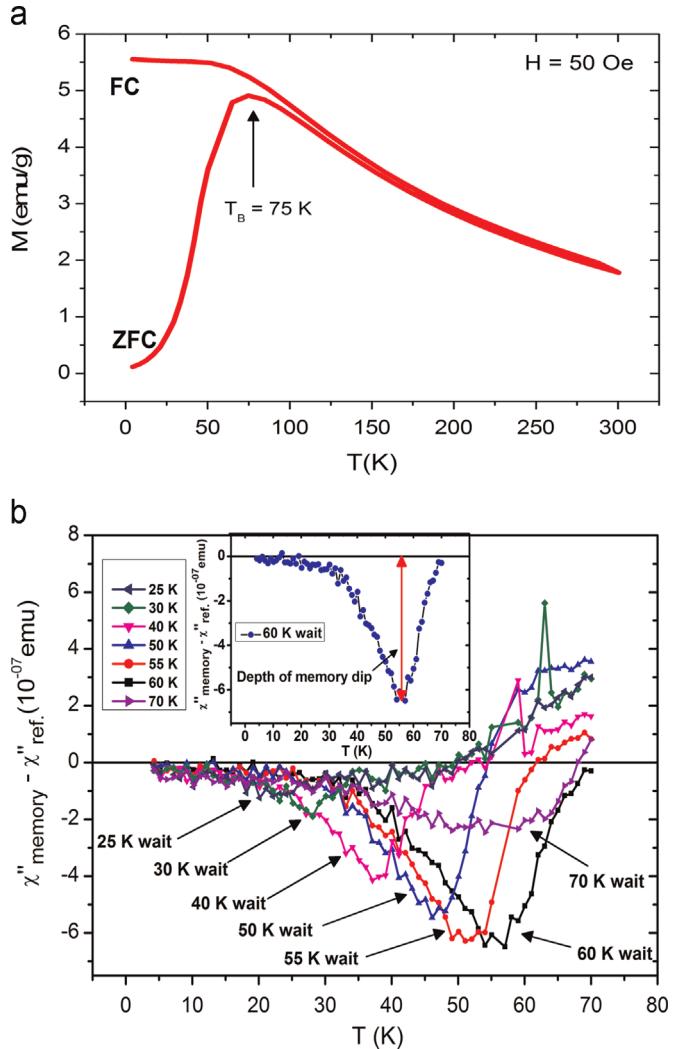

Fig. 2. (a) ZFC/FC magnetization curves of maghemite nanoparticles. Arrow indicates the average blocking temperature of the nanoparticles, (b) ME measured for different halted temperatures. The sample was halted at 25 K, 30 K, 40 K, 50 K, 55 K, 60 K, and 70 K for 2 h during the ZFC process to get χ''_{memory}, whereas the $\chi''_{ref.}$ is determined without any halting temperature. Inset shows that how the ME dip was calculated and vertical arrow indicates the depth of the ME dip.

due to large surface to volume ratio. The surface atoms have coordination bonds on the inner side only and thus contribute to surface disorder and magnetic frustration. Due to randomly frozen surface spins, the surface anisotropy is different as compared to core anisotropy of ferrimagnetically aligned core spins. The surface disorder and frustration are main ingredients for surface spin glass behavior. As core/shell interactions are usually dominant below T_B, we have chosen a region just below this temperature for ME and EB experiments.

The ME in ZFC magnetic measurement is a finger print for the spin glass behavior. Although we observed the ME in both in phase (see Fig. S1) and out of phase AC susceptibility, it appeared more pronounced in out of phase part. Therefore we have taken the out of phase AC susceptibility here. We adopted the ME measurement protocol as described in detail elsewhere [30]. To investigate the ME, one needs two curves, (i) the reference curve and (ii) the memory curve (for which the system is halted at particular temperature for a specified time). The difference between ZFC memory and ZFC reference curves shows a dip at the halting temperature which indicates the presence of ME as known from spin glass systems [30]. For the reference curve, the sample is continuously ZFC from room temperature to 4.2 K and then immediately the out of phase AC susceptibility is recorded on increasing temperature up to 70 K. For the memory curve, the

sample is also ZFC to a certain waiting temperature and halted there for some specific time (in our case 2 h). After this, the cooling is resumed to 4.2 K and the out of phase AC susceptibility is recorded on increasing temperature up to 70 K. The ZFC cooling rate was maintained at 5 Kpm (Kelvin per minute) for all the curves. The same unique reference curve was subtracted from all the memory curves.

Fig. 2(b) shows the difference of a memory and reference curves for different halting temperatures (25 K, 30 K, 40 K, 50 K, 55 K, 60 K and 70 K) for an AC field amplitude (H_{ac}) = 5 Oe and a frequency (f) = 10 Hz in the temperature range 4.2 70 K. The cor responding dip in the vicinity of the halted temperature is the signature of the ME in the sample due to spin glass behavior. The ME dip is shifted towards low temperatures as the halted tem perature is lowered [31]. The strength of ME can be interpreted in terms of the depth of the memory dip. The ME dip gets broadened and more pronounced at high temperatures. The collapse of the ME dip at 70 K halting temperature is due to the de blocking of the huge core spins and surface spins near the T_B of the nanoparticles.

For the measurement of the T dependence of the EB coupling, we cooled the sample under applied field of 5 T from 300 K to the desired temperature, and finally the M H loop was taken for a maximum applied field sweep of ± 5 T. Fig. 3(a) shows the var iation of the EB field (H_{exc}) and the depth of the ME dip with temperature. The horizontal shift of the M H loop after FC (5 T) was observed due to the presence of EB in these nanoparticles as demonstrated in the inset of Fig. 3(a). The EB effect in ferrite na noparticles originates from core/shell interactions due to FM aligned core spins and disordered frozen surface spins [32]. Below 30 K, the surface spins get blocked in their anisotropy axes and core/shell interactions develop. These core/shell interactions in crease with decreasing temperature due to decrease in thermal fluctuations and hence EB increases below 30 K. Above 30 K, these core/shell interactions decrease due to de blocking of surface spins and EB vanishes above 30 K (see Fig. S2) [33].
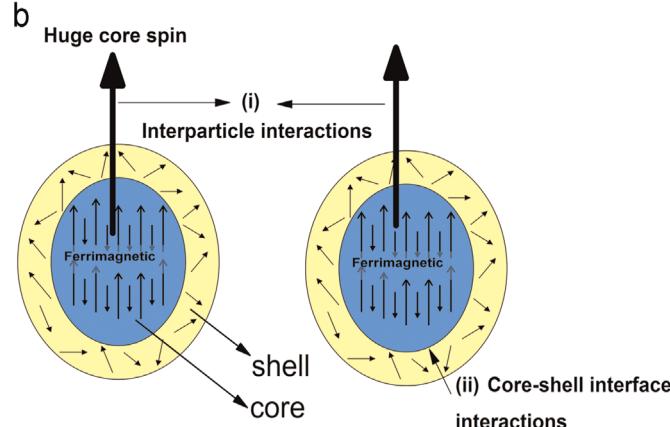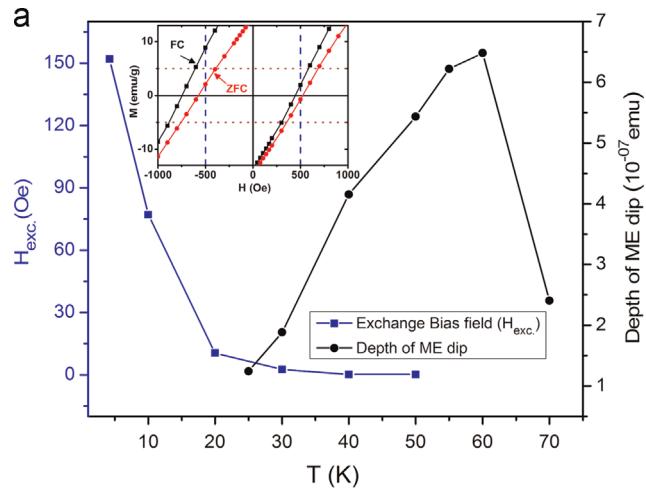
On the other hand, the depth of the ME dip decreases with lowering temperature and nearly vanishes at 25 K. Suzuki et al. [34] reported the T dependent ME in surfactant coated Fe_3O_4 na noparticles and found increase of depth of ME dip with decreasing temperature. Similar T dependent ME were also reported by Jönsson et al. [35] for Ag (11 at% Mn) system. In our case, the collapse of the ME dip occurs in the same temperature region in which the exchange bias starts developing. In nanoparticles, the ME can be due to two reasons; one is the super spin glass and other is surface spin glass behavior. Fig. 3(b) shows the demon stration of (i) interparticle interactions and (ii) core/shell interface interactions in individual nanoparticle. The interparticle interac tions are responsible for super spin glass behavior, while core/ shell interface interactions are responsible for surface spin glass behavior. The ME related to the surface spin glass is a very weak effect, which is dominated only at lower temperatures due to frozen blocked surface spins. However, ME due to super spin glass is dominated at higher temperatures and vanishes near T_B due to de blocking of the huge core spins of the individual nanoparticles. The mutual turn on/off of both competing effects coincides near a temperature of 25 30 K. The interface interactions at the core/ shell boundary of the nanoparticles stiffens the spin canting and thus diminishing the ME. This suggests that the weak core/shell interactions at the nanoparticle's surface do not enhance the ME as compared to system containing FM Co nanoparticles dispersed in AFM Mn matrix having strong FM/AFM interface interactions as reported by Vasilakaki et al. [21]. An explanation could be that our microwave deposited nanoparticles are not embedded in an AFM matrix, but act rather as single objects with interparticle (dipolar) interactions. For FM nanoparticles/AFM matrix, a collectively or dered AFM matrix would exert a long range EB field. In contrast, for loosely ordered (or random) nanoparticles the EB effect is more or less restricted to individual particles in which spin canting is the predominant coupling mechanism across the core/shell in terface. This is also the reason that only a small EB shift is observed in the hysteresis loops in our case. Therefore Fig. 3 should imply that the memory and exchange bias effects in these maghemite nanoparticles would be either counteracting processes OR scarcely overlapping, nearly independent phenomena.

4. Conclusions

We compared the temperature dependent EB and ME in ma ghemite nanoparticles. TEM image shows that the nanoparticles are spherical in shape and have narrow particle size distribution. ZFC/FC measurements reveal a well defined T_B of the nano particles at T = 75 K. The EB effect is reduced with increasing temperature and nearly vanishes at 30 K, which is attributed to decoupling of surface spins from core spins at the core shell in terface. The nanoparticles exhibit ME in ZFC process, which de creases with decreasing temperature and nearly vanishes at 25 K. Therefore both EB and ME vanish in a temperature range of 25 30 K. The EB causes spin canting at the core/shell interface and diminishes the ME as the temperature decreases. A stiffened random spin canting suppresses obviously memory and aging ef fects and reduces the EB shift of the hysteresis curve. In conclu sion, the EB effect due to core/shell interface interactions does not enhance ME but actually appears to decrease it due to spin canting at low temperatures.

Fig. 3. (a) Variation of the exchange bias field (H_{exc}) and depth of ME dip with temperature. Inset shows the coercivity region of M–H loops taken at 4.2 K for ZFC and FC processes. The FC M–H loop is horizontally shifted to left which demon strate the EB effect, (b) demonstration of (i) interparticle interactions and (ii) core/ shell interface interactions.

References

[1] A.P. Young, Spin Glasses and Random Fields (Series on Directions in Condensed Matter Physics Vol. 12), World Scientific, Singapore, 1998.

[2] T. Jonsson, J. Mattsson, C. Djurberg, F.A. Khan, P. Nordblad, P. Svedlindh, Aging in a magnetic particle system, Phys. Rev. Lett. 75 (1995) 4138.

[3] G.M. Tsoi, U. Senaratne, R.J. Tackett, E.C. Buc, R. Naik, P.P. Vaishnava, V.M. Naik, L.E. Wenger, Memory effects and magnetic interactions in a γ-Fe$_2$O$_3$ nanoparticle system, J. Appl. Phys. 97 (2005).

[4] K. Jonason, E. Vincent, J. Hammann, J.P. Bouchaud, P. Nordblad, Memory and chaos effects in spin glasses, Phys. Rev. Lett. 81 (1998) 3243.

[5] S. Sahoo, O. Petracic, W. Kleemann, P. Nordblad, S. Cardoso, P.P. Freitas, Aging and memory effect in a superspin glass, Phys. Rev. B 67 (2003) 214422.

[6] M. Bandyopadhyay, S. Dattagupta, Memory in nanomagnetic systems: superparamagnetism versus spin-glass behavior, Phys. Rev. B 74 (2006) 214410.

[7] Y. Sun, M.B. Salamon, K. Garnier, R.S. Averback, Memory effects in an interacting magnetic nanoparticle system, Phys. Rev. Lett. 91 (2003) 167206.

[8] V. Markovich, I. Fita, A. Wisniewski, G. Jung, D. Mogilyansky, R. Puzniak, L. Titelman, G. Gorodetsky, Spin-glass-like properties of La$_{0.8}$Ca$_{0.2}$MnO$_3$ nanoparticles ensembles, Phys. Rev. B 81 (2010) 134440.

[9] K. Hiroi, H. Kura, T. Ogawa, M. Takahashi, T. Sato, Spin-glasslike behavior of magnetic ordered state originating from strong interparticle magnetostatic interaction in α-Fe nanoparticle agglomerate, Appl. Phys. Lett. 98 (2011) 252505.

[10] J.L. Dormann, D. Fiorani, R. Cherkaoui, E. Tronc, F. Lucari, F. D'Orazio, L. Spinu, M. Noguès, H. Kachkachi, J.P. Jolivet, From pure superparamagnetism to glass collective state in Fe$_2$O$_3$ nanoparticle assemblies, J. Magn. Magn. Mater. 203 (1999) 23–27.

[11] W. Luo, S.R. Nagel, T.F. Rosenbaum, R.E. Rosensweig, Dipole interactions with random anisotropy in a frozen ferrofluid, Phys. Rev. Lett. 67 (1991) 2721.

[12] V. Bisht, K.P. Rajeev, Memory and aging effects in NiO nanoparticles, J. Phys.: Condens. Matter 22 (2010) 016003.

[13] K. Nadeem, H. Krenn, T. Traussing, I. Letofsky-Papst, Distinguishing magnetic blocking and surface spin-glass freezing in nickel ferrite nanoparticles, J. Appl. Phys. 109 (2011) 013912.

[14] M. Sasaki, P.E. Jonsson, H. Takayama, H. Mamiya, Aging and memory effects in superparamagnets and superspin glasses, Phys. Rev. B 71 (2005) 104405.

[15] D. De, K. Dey., S. Majumdar, S. Giri, Aging effects in nanocrystalline Co$_{50}$Ni$_{50}$ and Fe$_{50}$Ni$_{50}$ alloy: role of magnetic anisotropy, Solid State Commun. 152 (2012) 1857–1861.

[16] K. Khan, P. Mandal, D. Prabhakaran, Memory effects and magnetic relaxation in single-crystalline La$_{0.9}$Sr$_{0.1}$CoO$_3$, Phys. Rev. B 90 (2014) 024421.

[17] C. Raj Sankar, S. Vijayanand, S. Verma, P.A. Joy, Direct comparison of the aging and memory effects of magnetic nanoclusters and nanoparticles, Solid State Commun. 141 (2007) 307–310.

[18] D. Peddis, M. Hudl, C. Binns, D. Fiorani, P. Nordblad, Aging experiments in a superspin glass system of Co particles in Mn matrix, J. Phys.: Conf. Ser. 200 (2010) 072074.

[19] N. Domingo, D. Fiorani, A.M. Testa, C. Binns, S. Baker, J. Tejada, Exchange bias in a superspin glass system of Co particles in Mn matrix, J. Phys. D: Appl. Phys. 41 (2008) 134009.

[20] R. Malik, N. Sehdev, S. Lamba, P. Sharma, A. Makino, S. Annapoorni, Magnetic memory effects in nickel ferrite/polymer nanocomposites, Appl. Phys. Lett. 104 (2014) 122407.

[21] M. Vasilakaki, K.N. Trohidou, D. Peddis, D. Fiorani, R. Mathieu, M. Hudl, P. Nordblad, C. Binns, S. Baker, Memory effects on the magnetic behavior of assemblies of nanoparticles with ferromagnetic core/antiferromagnetic shell morphology, Phys. Rev. B 88 (2013) 140402(R).

[22] J. Nogués, Ivan K. Schuller, Exchange bias, J. Magn. Magn. Mater. 192 (1999) 203–232.

[23] V. Skumryev, S. Stoyanov, Y. Zhang, G. Hadjipanayis, D. Givord, J. Nogués, Beating the superparamagnetic limit with exchange bias, Nature 423 (2003) 850–853.

[24] J. Nogues, J. Sort, V. Langlais, V.S. Skumryev, J.S. Surinach Munoz, M.D. Baro, Exchange bias in nanostructures, Phys. Rep. 422 (2005) 65–117.

[25] R. Cabreira-Gomes, F.G. Silva, R. Aquino, P. Bonville, F.A. Tourinho, R. Perzynski, J. Depeyrot, Exchange bias of MnFe$_2$O$_4$ @ γ-Fe$_2$O$_3$ and CoFe$_2$O$_4$ @ γ-Fe$_2$O$_3$ core/shell nanoparticles, J. Magn. Magn. Mater. 368 (2014) 409–414.

[26] D. Vollath, D.V. Szabo, The microwave plasma process – a versatile process to synthesize nanoparticulate materials, J. Nanopart. Res. 8 (2006) 417–428.

[27] D. Vollath, D.V. Szabo, R.D. Taylor, J.O. Willis, Synthesis and magnetic properties of nanostructured maghemite, J. Mater. Res. 12 (1997) 2175–2182.

[28] K. Nadeem, H. Krenn, T. Traussnig, R. Wurschum, D.V. Szabo, I. Letofsky-Papst, Spin-glass freezing of maghemite nanoparticles prepared by microwave plasma synthesis, J. Appl. Phys. 111 (2012) 113911.

[29] K. Nadeem, H. Krenn, W. Sarwar, M. Mumtaz, Comparison of surface effects in SiO$_2$ coated and uncoated nickel ferrite nanoparticles, Appl. Surf. Sci. 288 (2014) 677–681.

[30] T. Jonsson, K. Jonason, P. Jonsson, P. Nordblad, Nonequilibrium dynamics in a three-dimensional spin glass, Phys. Rev. B 59 (1999) 8770.

[31] R. Mathieu, P.E. Jonsson, P. Nordblad, H.A. Katori, A. Ito, Memory and chaos in an ising spin glass, Phys. Rev. B 65 (2001) 012411.

[32] R.H. Kodama, A.E.E. Berkowitz, J. Mcniff, S. Foner, Surface spin disorder in NiFe$_2$O$_4$ nanoparticles, Phys. Rev. Lett. 77 (1996) 394–397.

[33] X. Sun, N.F. Huls, A. Sigdel, S. Sun, Tuning exchange bias in core/shell FeO/Fe$_3$O$_4$ nanoparticles, Nano Lett. 12 (1) (2012) 246–251.

[34] M. Suzuki, S.I. Fullem, I.S. Suzuki, L. Wang, C.J. Zhong, Observation of superspin-glass behavior in Fe$_3$O$_4$ nanoparticles, Phys. Rev. B 79 (2009) 024418.

[35] P.E. Jönsson, R. Mathieu, P. Nordblad, H. Yoshino, H.A. Katori, A. Ito, Examination of the ghost domain scenario non-equilibrium dynamics of spin glasses, Phys. Rev. B 70 (2004) 174402.